Clays and Clay Minerals, Vol. 41, No. 3, 365–372, 1993.

LOW TEMPERATURE EXPERIMENTAL INVESTIGATION OF THE EFFECT OF HIGH pH KOH SOLUTIONS ON THE OPALINUS SHALE, SWITZERLAND

J. A. CHERMAK

Mineralogisch-Petrographisches Inst., Universtät Bern Baltzerstrasse 1, CH - 3012 Bern, Switzerland

Abstract—Batch reactor experiments were performed at 150°C, 175°C, and 200°C to determine the effect of high pH KOH solutions on the mineralogy of the Opalinus shale. In these experiments, the change in solution quench pH at 25°C, solution composition, and mineralogy were monitored as a function of time for up to ≈50 days. Runs were performed in 50 ml titanium hydrothermal reactor vessels. Each reactor was charged with 0.5–5.0 grams of the 80–200 mesh size fraction of Opalinus shale, and 25 ml of solution (0.08 and 0.008 m KOH). Under these high pH conditions, the general sequence of reaction products observed is the formation of phillipsite, followed by K-feldspar ± K-rectorite. Phillipsite is a metastable intermediate that eventually transforms to K-feldspar. This sequence of mineral reaction products is very different from that found in the NaOH system.

Key Words—Experimental investigation, High pH, K-rectorite, K-feldspar, Opalinus shale, Phillipsite.

INTRODUCTION

High pH solution-mineral reactions occur naturally in a variety of geological environments and also where the environment has been modified by various engineering projects. The occurrence and types of these high pH-mineral reactions are discussed in detail in Chermak (1992). Particularly applicable to the present study is the interaction of high pH K dominated cement pore fluids with shales. There are many field studies that show the formation of zeolites, potassium feldspar, and clay minerals in the high pH K dominant system (Hay, 1978, 1986; Peaver *et al.,* 1980; Velde, 1985; Hower *et al.,* 1976). The precipitation of zeolites and clay minerals under high pH K dominant conditions has also been documented in the laboratory, although very little experimental data exists on the effects of the interaction of these solutions with shales. This present experimental investigation examines the effect of high pH KOH solutions on the Opalinus shale (middle Jurassic, Mont Terri, Northern Switzerland).

Previous experimental studies conducted under high pH conditions using different starting materials, over a range of temperatures, pHs and solution compositions have produced zeolites, K-feldspar, and clays (Barrer, 1982). Focusing on the K dominant system, varying types of zeolites have been observed to grow and precipitate (Donahoe *et al.,* 1984; Donahoe and Liou, 1985; Hawkins, 1981; Hawkins *et al.,* 1978). Especially applicable to this study are those experiments conducted by Barth-Wirshing and Höller (1989) where their starting material was rhyolitic glass and the precipitation of phillipsite was observed in KOH solutions. K-feldspar stability relations in the K_2O-Al_2O_3-SiO_2-H_2O system have been described by Hemley (1959) and Hess (1966). Experimental clay mineral transformations in shales have also been widely studied in the laboratory (Eberl, 1978; Velde, 1985; Matsuda and Henmi, 1983; Whitney and Northrop, 1988). Directly applicable to this study is the work of Eberl (1978) and Matsuda and Henmi (1983), where the formation of K-rectorite was observed.

To investigate mineralogical alterations when shales are in contact with high pH KOH solutions, experiments were conducted at 150°C, 175°C, and 200°C using the Opalinus shale. In these experiments, both solids and solutions were monitored as a function of time to determine changes that occur in the solution and in the mineralogy of the shale.

EXPERIMENTAL METHODS

Batch experiments were run in 50 ml titanium hydrothermal reactor vessels, the detail and design of which are given in Chermak and Rimstidt (1990). These reactors were sealed and placed onto a rotisserie unit (8 rpm) inside an oven set at temperatures of 150°C, 175°C, or 200°C for reaction times of up to 51 days. Each reactor was charged with variable amounts (0.5–5.0 grams) of the 80–200 mesh size fraction of Opalinus shale and 25 ml of solution of varying KOH composition (0.08–0.008 m). The specific surface area of the starting solid was calculated from a N_2 desorption BET isotherm to be 14.7 m^2/g. The total organic matter in the shale is < 0.5 wt. % as determined by coulometric methods. Individual reactors were removed at specific intervals, quenched in cold water, and opened. The

---

Present address: Department of Geology, Georgia State University, 340 Kell Hall, Atlanta, Georgia 30303.

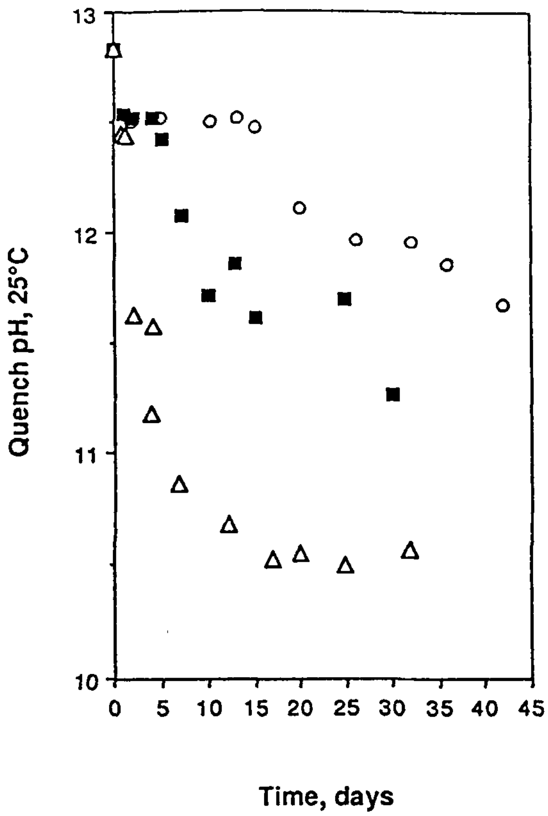

Figure 1. A plot of quench pH at 25°C *vs* time in days for 0.08 m KOH experiments at 150°C (open circles), 175°C (solid squares), and 200°C (open triangles).

solution pH was measured at 25°C using a Ross combination pH electrode, and the solids were separated from the solution by centrifugation and then decanting the solution. The solution was filtered through a 0.45 μm filter and saved for further analysis. The solids were then washed with distilled/deionized water and saved for X-ray diffraction analysis.

Dissolved K and Si concentrations were determined for all samples and Ca, Mg, Al, and Fe for select runs. K concentration in solution was determined by atomic absorption spectrophotometry (AAS) using a CsCl ionization buffer (Varian, 1979). In select samples (175°C run), K was determined by ion chromatography (I.C.) and differed from the AAS values by < 5%. I.C. was also used to determine Mg and Ca concentrations for all samples in the 175°C run. Mg values were below 5 ppm for all samples. Silica concentrations were determined colorimetrically using the molybate blue method (Govett, 1961; Gieskes and Peretsman, 1986). Al concentration in solution was determined (7 and 25 days at 175°C) by ion coupled plasma spectrophotometry (ICP) and was found to be very low and close to the detection limit of the instrument (0.5 ppm). In select samples, Fe in solution was measured by the Dipiridal colorimetric method (E. Merck AG, 1966) and was found to be below the detection limit (0.2 ppm).

The Opalinus shale was characterized by X-ray diffraction (XRD), X-ray fluorescence (XRF), scanning electron microscopy (SEM), and surface area analysis. Reaction products were examined by XRD (CuKα radiation) and SEM. The Ca saturated, < 4 μm fraction (this fraction appeared to have the largest amount of reaction products) was prepared by the millipore method (Moore and Reynolds, 1989) and utilized for XRD analysis. Further splits in the < 4 μm fraction (< 2 μm and minerals between 2 μm and 4 μm) were conducted to better characterize reaction products. Patterns were collected for air dried, glycolated, and heat treated (550°C for 1 hr) samples. To characterize the nature of the expandable phase of the K-rectorite, further diffraction patterns were collected after Mg saturation and exposure to both glycol and glycerol. To confirm identification of the zeolite phase, a Guinier type camera was used (FeKα_1 radiation). XRD determination of the amount of quartz and calcite was done on the bulk shale using a LiF internal standard mixture (Brindley, 1980), and semi-quantitative analysis of the < 4 μm fraction was determined by comparing patterns to those of standard clay mineral mixtures (Snyder and Bish, 1989; Brindley, 1980; Pawloski, 1985). Quantitative determination of mineral phases in shales is quite difficult; in this study, only relative changes in mineral proportions are discussed (i.e., total disappearance of diffraction peaks and appearance of new peaks). The mineral composition of the starting shale is approximately 40% quartz, 20% kaolinite, 15% muscovite (illite), 15% calcite, 5% chlorite, 3% mixed layer illite/smectite, 2% siderite, and a trace of pyrite. The values of siderite and pyrite were derived by estimates using optical mineralogy. The chemical composition of the starting Opalinus shale as determined by XRF is given in Chermak (1992). SEM was used to examine crystal habit and morphology and to aid in confirming reaction products.

RESULTS

Table 1 gives the quench pH at 25°C, and K, Si and Ca (175°C only) concentration *vs* time data at 150°C, 175°C, and 200°C for six experiments. These experiments evaluate the effect of temperature (150°C, 175°C, and 200°C with 0.5 g solid and 25 ml of 0.08 m KOH solution), solid/solution ratio (200°C with 0.5, 1.5, and 5.0 g of solid), and solution composition (200°C with 0.5 g solid and 25 ml of 0.08 m and 0.008 m KOH solution) on the transformations occurring as a function of time in the Opalinus shale. Figure 1 shows a plot of quench pH at 25°C *vs* time at 150°C, 175°C, and 200°C. Notice the pH shoulder that occurs at pH ≈ 12.50; this will be discussed later. Notice also the large effect at 200°C that the amount of shale has on

Table 1. Quench pH at 25°C and K, Ca (175°C only), and Si concentration *vs.* time data at 150°C, 175°C, and 200°C.

Time, days	pH 25°C	K, ppm	Silica, ppm	Ca, ppm
150°C, 0.08 m KOH, 0.5 g				
0.000	12.83	3130	0	
1.844	12.50	2480	190	
4.948	12.51	2448	202	
10.104	12.50	2249	151	
13.000	12.51	2259	143	
15.135	12.47	2258	177	
20.031	12.11	2081	778	
26.031	11.97	2129	734	
31.938	11.96	1996	645	
35.896	11.86	2012	630	
41.948	11.67	2046	611	
175°C, 0.08 m KOH, 0.5 g				
0.000	12.83	3130	0	0
1.000	12.53	2445	228	31
2.000	12.51	2447	217	33
4.000	12.51	2462	175	0
5.042	12.42	2213	225	35
7.031	12.08	2119	710	2.0
10.000	11.71	2157	720	0.0
12.740	11.86	1991	699	0.0
15.052	11.61	2057	648	0.0
24.792	11.70	1764	518	2.0
30.000	11.26	1785	545	0.0
200°C, 0.08 m KOH, 0.5 g				
0.000	12.83	3130	0	
0.833	12.45	2283	356	
1.250	12.44	2128	248	
2.062	11.63	2176	777	
3.792	11.18	2084	705	
4.000	11.58	1820	727	
6.771	10.86	1860	613	
11.917	10.68	2105	513	
16.917	10.53	1964	467	
19.917	10.55	2067	477	
24.771	10.50	1981	460	
31.750	10.46	1904	443	
200°C, 0.08 m KOH, 1.5 g				
0.000	12.83	3130	0	
0.875	12.18	2116	135	
2.896	12.05	1991	96	
3.771	10.50	1266	336	
5.104	10.52	1142	362	
7.125	10.34	1126	289	
11.833	10.39	671	251	
15.833	10.07	1034	165	
19.104	10.02	963	150	
26.094	9.84	487	134	
31.979	9.66	871	101	
51.052	9.58	589	104	
200°C, 0.08 m KOH, 5 g				
0.000	12.83	3130	0	
2.156	8.37	1006	23.4	
5.167	7.97	874	70.9	
12.885	7.57	908	56.9	
21.083	7.57	543	55.2	
31.979	7.68	662	55.2	

Table 1. Continued.

Time, days	pH 25°C	K, ppm	Silica, ppm
200°C, 0.008 m KOH, 0.5 g			
0.000	11.88	313.0	0
0.916	7.41	—	45.7
3.188	6.93	202.9	70.5
5.167	6.50	196.4	76.1
7.875	6.29	191.0	67.8
10.802	6.30	187.7	69.9
14.812	6.25	180.2	65.2
19.062	6.38	189.6	69.0
26.917	6.43	184.6	65.0
43.990	6.51	177.7	64.0

—, not determined.

the solution pH, indicating a substantial buffering capacity (Table 1).

The determined K and Si values (Table 1) showed precision errors (reproducibility) of < 4% using AAS and < 3% using colorimetric methods, respectively. A general decreasing trend in K can be observed in these experiments, although the K data is a bit erratic. This can possibly be explained by contamination during the measurement of pH with a KCl electrode (3.0 M filling solution) or by the presence of K-rectorite, which has

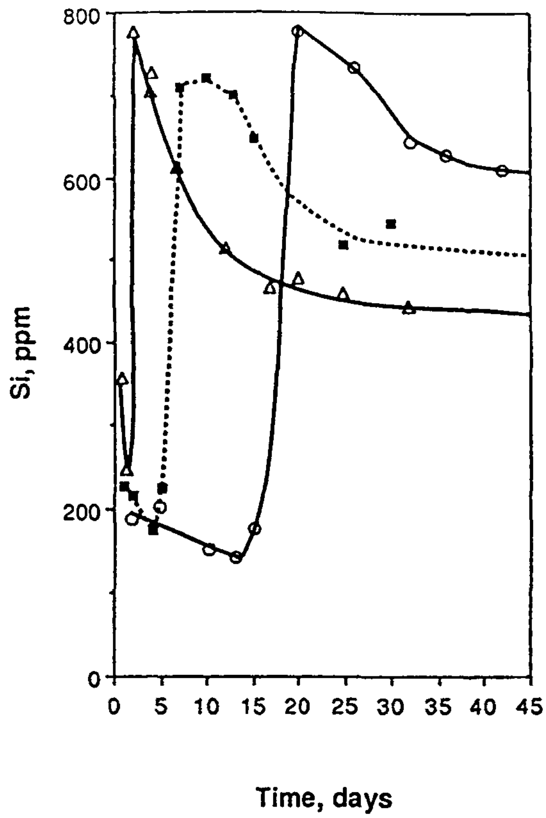

Figure 2. A plot of Si concentration, ppm *vs* time in days for 0.08 m KOH experiments at 150°C (open circles), 175°C (solid squares), and 200°C (open triangles).

https://doi.org/10.1346/CCMN.1993.0410313 Published online by Cambridge University Press

Table 2. Reaction products of the < 4 μm fraction *vs.* time data at 150°C, 175°C, and 200°C as determined by XRD.

Time, days	Reaction products
	150°C, 0.08 m KOH, 0.5 g
1.844–13.000	no change
15.135–20.031	phillipsite
26.031	phillipsite, K-feldspar
31.938–41.948	phillipsite, K-feldspar, K-rectorite
	175°C, 0.08 m KOH, 0.5 g
1.000–4.000	no change
5.042–7.031	phillipsite
10.000–24.792	phillipsite, K-feldspar, K-rectorite
30.000	K-feldspar, K-rectorite
	200°C, 0.08 m KOH, 0.5 g
0.833–1.250	phillipsite
2.062–6.771	phillipsite, K-feldspar, K-rectorite
11.917	K-feldspar, K-rectorite, muscovite/muscovite
16.917–31.750	K-feldspar, muscovite/muscovite
	200°C, 0.08 m KOH, 1.5 g
0.875–2.896	no change
3.771–7.125	phillipsite
11.833–15.833	phillipsite, K-feldspar
19.104–51.052	K-feldspar
	200°C, 0.08 m KOH, 5 g
2.156–31.979	no change
	200°C, 0.008 m KOH, 0.5 g
0.917–43.990	no change

the ability to exchange K. Silica data for 150°C, 175°C, and 200°C runs are plotted in Figure 2 and show a range of values from 140–780 ppm.

Along with changes in solution composition with time, mineralogical transformations were monitored. Experimental reaction products found in the < 4 μm fraction, as determined by XRD are given in Table 2. A general sequence of events observed at all temperatures in the 0.5 g experiments include first the precipitation of phillipsite, followed by K-feldspar ± K-rectorite precipitation. To further characterize the zeolite phase, a Guinier type camera was used. Distinguishing different types of zeolites in mineral mixtures can be very difficult, and Donahoe *et al.* (1984) describe in detail how to distinguish phillipsite from merlinoite using XRD. Results from observation with a Guinier type camera showed a characteristic phillipsite peak at ≈4.15 Å as well as the absence of a sharp 4.5 Å zeolite peak indicative of merlinoite.

Figure 3 shows four X-ray diffraction patterns of the Ca saturated, ethylene glycol solvated < 4 μm fraction of the starting Opalinus clay and products at 175°C. This sequence shows first the presence of phillipsite precipitated after 7 days, followed by that of K-feldspar and K-rectorite after 13 days, and finally the absence of phillipsite in the 30-day experiment. Reaction products at 175°C were also examined with SEM and Figure 4 shows the development of phillipsite prisms after ≈7 days, and the clay morphology of K-rectorite after ≈25

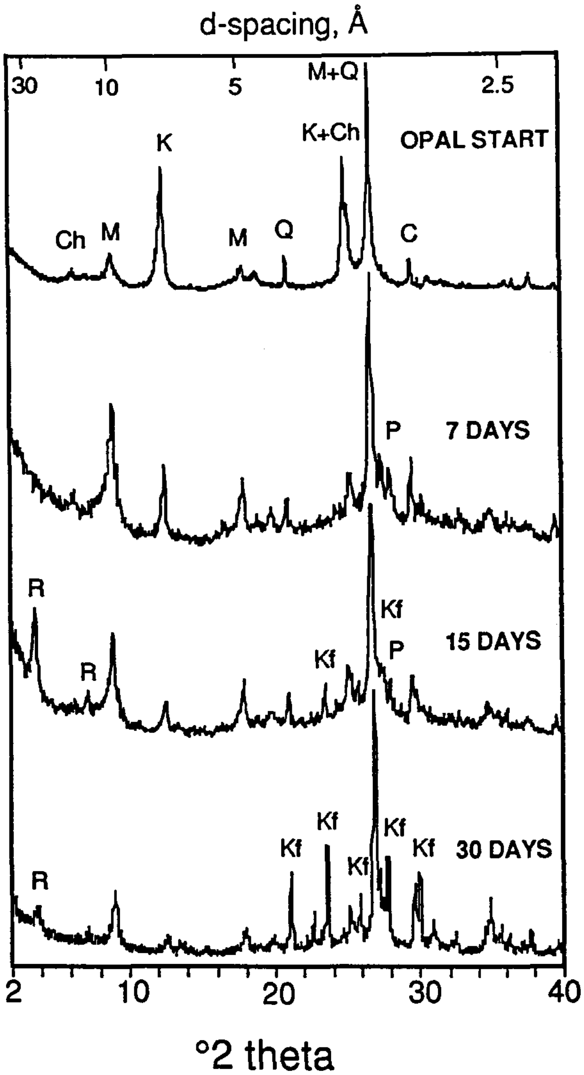

Figure 3. X-ray diffraction patterns of the Ca saturated, ethylene glycol solvated < 4 μm fraction of the Opalinus shale. The top pattern is the starting shale, and the bottom three are the shale reacted with 0.08 m KOH solution at 175°C after ≈7, ≈15, and 30 days. Labels on the XRD peaks correspond to Ch = chlorite, K = kaolinite, M = muscovite, Q = quartz, C = calcite, P = phillipsite, Kf = K-feldspar, and R = K-rectorite.

days. The K-rectorite phase expanded from ≈22.4 Å (Ca saturated, air dried) to ≈24.9 Å when exposed to glycol, and collapsed to 10 Å when heat treated at 550°C. K-rectorite showed no expansion (d(001) at ≈22.4 Å) after being Mg saturated and exposed to both glycol and glycerol. The transformation of phillipsite to K-feldspar was also observed with the SEM (Figure 5). Figures 5a–5c show a close-up of the phillipsite prisms developed after 2 days as well as the typical texture of K-feldspar and a close-up of these grains as shown by the white arrows (5c). The significance of this transformation will be discussed later.

In the 0.5 g, 200°C experiment for times longer than

https://doi.org/10.1346/CCMN.1993.0410313 Published online by Cambridge University Press

≈7 days, the precipitation of a mixed layer mica/mica mineral composed of two types of mica is observed. It seems reasonable to assume that both mica layers are K micas because the solution chemistry is dominated by K. Figure 6 shows the sequence of development of this mineral in the < 2 μm fraction (Ca saturated, glycolated), as monitored by XRD. The mineral is identified as a mixed layer mica/mica because of the presence of a 19.8 Å peak. This peak is interpreted to result from a compositional superlattice, which is probably produced by significantly different Fe contents of the two mica types. Also shown in Figure 6 is the mineral phase distribution as a function of grain size for the ≈12 and ≈17 day experiments.

Initial experiments were also conducted with the Opalinus shale in contact with a mixed Na/K hydroxide solution (0.05 m NaOH and 0.04 m KOH, starting pH = 12.85). The amount of starting Na and K in solution is quite an important parameter, and it must be emphasized that these are initial results for only one Na/K solution ratio. Experiments were run at both 150°C and 175°C for run times up to ≈42 days. In the 150°C and 175°C experiments after ≈42 and ≈30 days, respectively, phillipsite, rectorite, and K-feldspar were observed in reaction products. Quench pH values were similar to the results in the 0.1 m Na system (Chermak, 1992).

To investigate mineralogical alterations when other shales are in contact with high pH NaOH and KOH solutions, experiments were conducted at 150°C using the Palfris Formation (lower Cretaceous, Eastern Switzerland, possible low level radioactive waste repository site). Starting minerals as determined by quantitative XRD are approximately 25% calcite, 20% quartz, 20% muscovite (illite), 16% mixed layer illite/smectite, 12% chlorite, and 7% ankerite. The reaction product Na-rectorite was observed by XRD in the 0.1 m NaOH experiments after 11 days and remained until the termination of the experiment (48 days). Due to the absence of kaolinite in the starting shale, the precipitation of analcime was not observed. In the 0.08 m KOH experiments, phillipsite and K-rectorite were detected after 22 days and phillipsite, K-feldspar and K-rectorite were observed after 48 days.

DISCUSSION

Combining the solution and solid data in the 150°C, 175°C, and 200°C experiments brings several details of the mineral transformations into focus. Initially, the dissolution of the primary silicates, kaolinite and quartz (as observed by XRD) contributes to the observed increase in silica concentration (Figure 2) and an associated drop in pH (Figure 1). After the initial pH drop, a pH shoulder is observed in the 150°C, 175°C, and 200°C experiments. The constant pH behavior is probably controlled by silica speciation, and will be discussed in detail later in this section. Eventually phillipsite is observed in the reaction products (Table 2). The precipitation of phillipsite and the corresponding decrease in the reactants kaolinite and quartz suggest that the first important reaction is kaolinite + quartz → phillipsite. The distribution of silica in this reaction is critical in determining what effect the precipitation of phillipsite has on solution pH. Three of the possible reactions in this system include:

$$3\,Al_2Si_2O_5(OH)_4 + 4\,H_4SiO_4 + 6\,K^+ + H_2O \rightarrow K_6Al_6Si_{10}O_{32}\cdot 12\,H_2O + 6\,H^+ \quad (1)$$

$$3\,Al_2Si_2O_5(OH)_4 + 4\,H_3SiO_4^- + 6\,K^+ + H_2O \rightarrow K_6Al_6Si_{10}O_{32}\cdot 12\,H_2O + 2\,H^+ \quad (2)$$

$$3\,Al_2Si_2O_5(OH)_4 + 4\,H_2SiO_4^{2-} + 6\,K^+ + 2\,H^+ + H_2O \rightarrow K_6Al_6Si_{10}O_{32}\cdot 12\,H_2O \quad (3)$$

In Reactions 1 and 2, K^+ is consumed and H^+ produced as phillipsite precipitates. In Reaction 3, however, H^+ is consumed as phillipsite precipitates. In the 0.08 m KOH, 150°C, 175°C, and 200°C experiments,

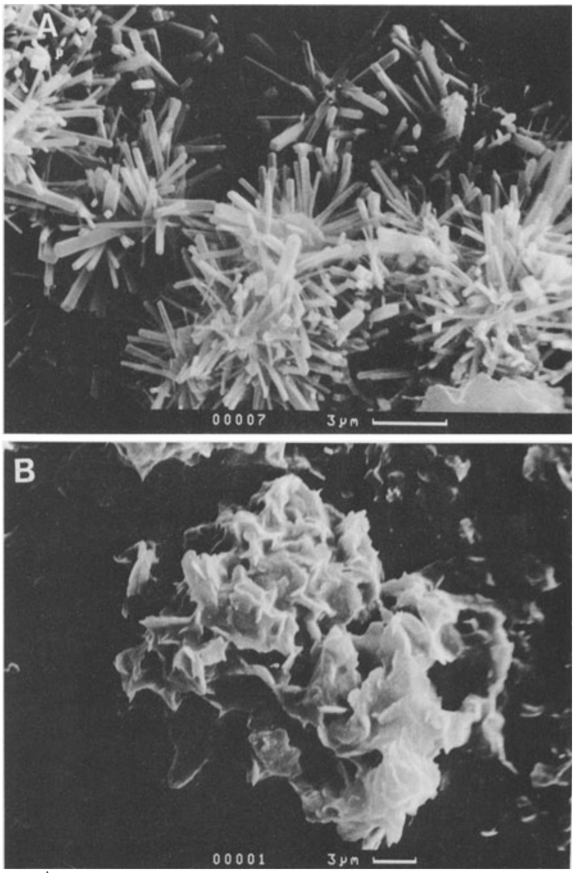

Figure 4. SEM photographs of reaction products at 175°C in contact with 0.08 m KOH solutions: A) phillipsite prisms that precipitated after ≈7 days; B) K-rectorite grains after 30 days.

https://doi.org/10.1346/CCMN.1993.0410313 Published online by Cambridge University Press

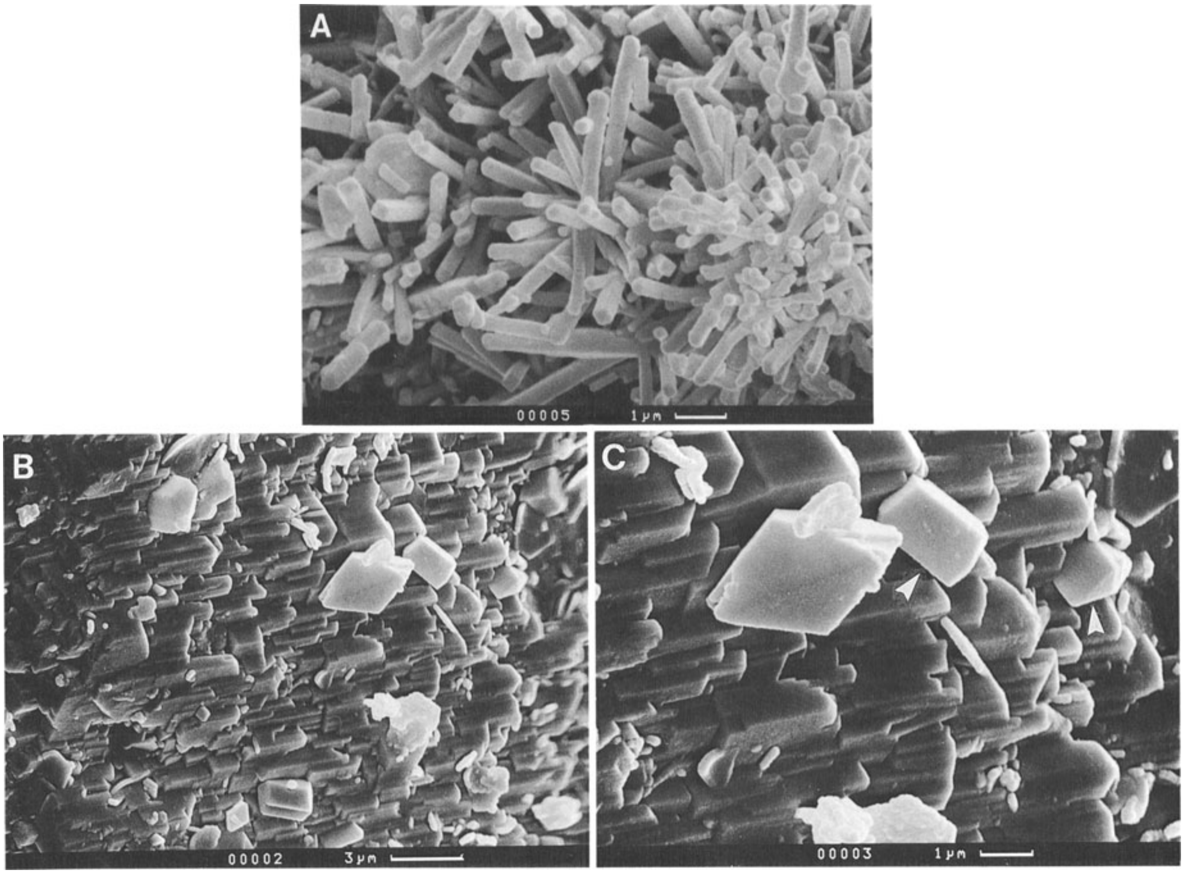

Figure 5. SEM photographs of reaction products at 200°C in contact with 0.08 m KOH solutions: A) phillipsite prisms that precipitated after 2 days; B) typical morphology of K-feldspar grains in the 25 day experiment; C) higher magnification photograph of the K-feldspar grains after ≈25 days shown by the white arrows.

the pH is observed to remain constant after phillipsite is first detected in the reaction products (Figure 1). This constant pH behavior can be explained by combining Reactions 2 and 3 to give the reaction:

$$3\,Al_2Si_2O_5(OH)_4 + 2\,H_2SiO_4^{2-} + 2\,H_3SiO_4^{-} + 6\,K^+ + H_2O \rightarrow K_6Al_6Si_{10}O_{32}\cdot 12\,H_2O \quad (4)$$

Kaolinite continues to react until it dissolves completely. Once the kaolinite has been used up, phillipsite precipitation stops, but the dissolution of quartz continues. This continued dissolution is demonstrated by the observed increase in Si concentration and decrease in pH (Table 2). This quartz dissolution behavior and solution response is explained by the reaction:

$$SiO_2 + 2\,H_2O \rightarrow H_3SiO_4^{-} + H^+ \quad (5)$$

The second mineral phase observed to precipitate in these experiments was K-feldspar. The appearance of K-feldspar coincided with a decrease in silica concentration of the solution (Table 1). The disappearance of phillipsite and the observed decrease in Si is consistent with the reaction:

$$K_6Al_6Si_{10}O_{32}\cdot 12\,H_2O + 8\,H_4SiO_4 \rightarrow 6\,KAlSi_3O_8 + 28\,H_2O \quad (6)$$

In the 175°C and 200°C experiments the complete transformation of phillipsite to K-feldspar (Figures 3 and 5) was observed. The formation of K-feldspar from phillipsite has been observed in nature (e.g., saline alkaline lakes) and is also described as a paragenetic sequence in geologic time (Hay, 1966). Phillipsite therefore is an intermediate phase in this transformation process.

The formation of K-rectorite coincides with the disappearance of chlorite, which is similar to results observed in the Na system (Chermak, 1992). This might have been an important transformation reaction, but the details of this reaction are quite complex and presently poorly understood. In the 0.5 gram, 200°C experiment the K-rectorite phase begins to transform into a mixed layer mica/mica phase after ≈12 days and continues until the K-rectorite totally transforms to mica/mica after ≈17 days (Figure 6). This mixed layer mica/mica mineral may have inherited its structure from the K-rectorite as the transformation occurred. The overall trend in clay mineral transformations from a K-rectorite to illite has also been postulated by Eberl and Hower (1977) and Eberl (1978), and has been described as the "mica trend."

Comparison of these experiments to those in the Na system (Chermak, 1992) enables some details of these high pH reactions to be discussed. In both systems, the kaolinite and quartz of the starting shale react to form zeolites (Na system : analcime; K system : phillipsite). The analcime in the Na system remains until the termination of the experiment, while the phillipsite transforms to K-feldspar in the K system. These results are consistent with observations of zeolitic assemblages in nature (Hay, 1966). In both the Na and K systems as well as the mixed Na/K system, a rectorite phase is observed and could be a very important phase that forms under high pH conditions in clay systems. Considering the solution data in both systems, the amount of Opalinus shale used has a large effect on the quench pH. However, there seems to be no simple relationship between surface area of the solid and the corresponding pH value. A pH shoulder is observed in the K system that is not observed in the Na system. Solution silica values for both the Na and K systems show a large decrease when the precipitation of rectorite and K-feldspar are observed.

Transformations that could occur when shales are in contact with high pH solutions must be considered to evaluate the safety of a repository. Starting shale mineralogy as well as solution chemistry has a large effect on the reactions that are observed. Understanding the interaction of the fluids associated with cement and their interaction with the host rock is essential. The precipitation of these zeolite and clay phases will alter properties of the host rock.

CONCLUSIONS

The main purpose of this experimental investigation was to determine the effect of high pH KOH solutions on the Opalinus shale. These high pH solutions are similar to those found in the pore waters of concrete, and these laboratory conditions simulate interactions that could occur in a repository environment where pore waters from the concrete interact with a host shale. Reactions of high pH KOH solutions with the Opalinus shale reduce the pH and significantly change the mineralogy of the shale. The general sequence of reaction products observed included first the precipitation of phillipsite, followed by K-feldspar ± K-rectorite. Starting minerals that were found to react include kaolinite, quartz, and chlorite.

Experiments conducted in the shale/high solution pH system can be used to constrain existing thermodynamic and kinetic models presently used in nuclear waste disposal. Experiments under these high pH conditions seem to show similar changes in mineralogy as found in other low pH, higher temperature studies although reaction rates in the high pH environments are much faster.

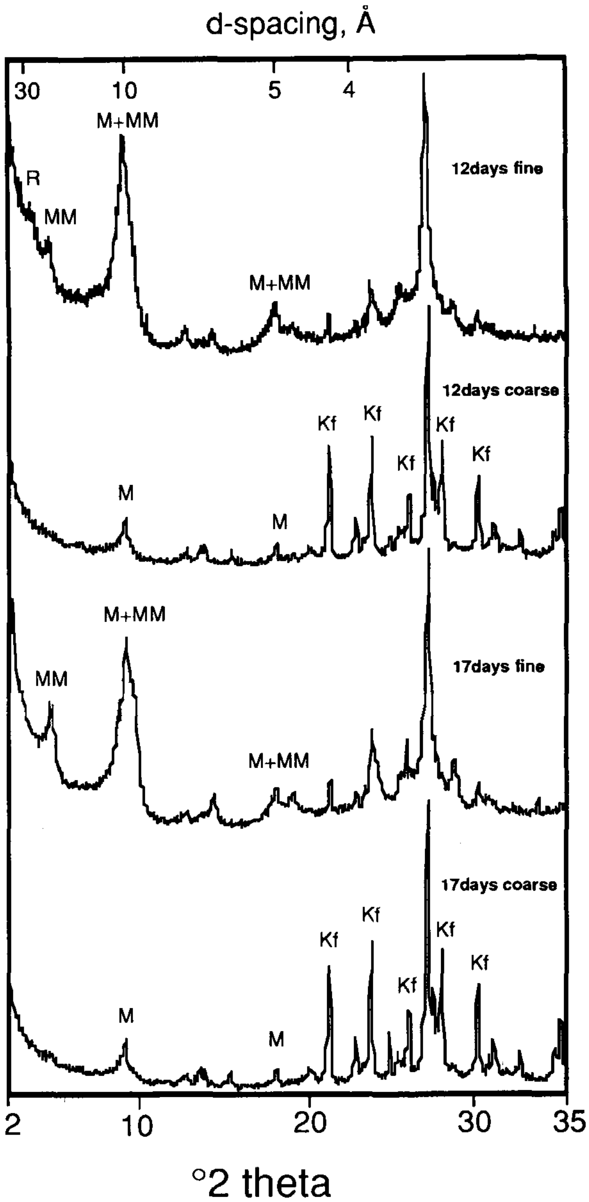

Figure 6. X-ray diffraction patterns of the Ca saturated, ethylene glycol solvated < 2 μm fraction of the Opalinus shale at 200°C after ≈12 and ≈17 days, showing the transformation of K-rectorite to mixed layer mica/mica as well as the size distribution of mineral phases (labeled coarse fraction minerals < 4 μm and > 2 μm). Note the distribution of reaction products is as would be expected with phillipsite and K-feldspar being found in greater proportions in the coarse fraction, while the < 2 μm fraction contains the interlayered clay minerals. Labels are the same as for Figure 3 with the addition of MM = mica/mica.

ACKNOWLEDGMENTS

Thanks are due to Tjerk Peters and the Mineralogy-Petrography Institute, University of Bern, for the funding of the present research. Helpful discussions and comments of early versions of this manuscript by Steve Hillier and Don Rimstidt are greatly appreciated. Discussions with Thomas Armbruster about zeolite structural analysis are greatly appreciated. Critical reviews and comments by Rona Donahoe and K. Tomita are gratefully acknowledged.

REFERENCES

Barrer, R. M. (1982) *Hydrothermal Chemistry of Zeolites:* Academic Press, New York.

Barth-Wirsching, U. and Höller, H. (1989) Experimental studies on zeolite formation conditions: *European Journal of Mineralogy* **1,** 489–506.

Brindley, G. W. (1980) Quantitative X-ray mineral analysis of clays: in *Crystal Structures of Clay Minerals and Their X-ray Identification,* G. W. Brindley and G. Brown, eds., Mineralogical Society, London, 411–438.

Chermak, J. A. (1992) Low temperature experimental investigation of the effect of high pH NaOH solutions on the Opalinus shale, Switzerland: *Clays & Clay Minerals* **40,** 650–658.

Chermak, J. A. and Rimstidt, J. D. (1990) The hydrothermal transformation rate of kaolinite to muscovite/illite: *Geochim. et Cosmochim. Acta* **54,** 2979–2990.

Donahoe, R. J., Liou, J. G., and Guldman, S. (1984) Synthesis and characterization of zeolites in the system Na_2O-K_2O-Al_2O_3-SiO_2-H_2O: *Clays & Clay Minerals* **32,** 433–443.

Donahoe, R. J. and Liou, J. G. (1985) An experimental study on the process of zeolite formation: *Geochim. et Cosmochim. Acta* **49,** 2349–2360.

Eberl, D. (1978) Reaction series for dioctahedral smectites: *Clays & Clay Minerals* **26,** 327–340.

Eberl, D. and Hower, J. (1977) The hydrothermal transformation of sodium and potassium smectite into mixed layer clay: *Clays & Clay Minerals* **25,** 215–227.

Gieskes, J. and Peretsman, G. (1986). Water Chemistry procedures aboard Joides Resolution—Some comments: *Ocean Drilling Program Technical Note No. 5,* Texas A&M University.

Govett, G. J. S. (1961) Critical factors in the colorimetric determination of silica: *Analytica Chimica Acta* **25,** 69–80.

Hawkins, D. B., Sheppard, R. A., and Gude, 3rd, A. J. (1978) Hydrothermal synthesis of clinoptilolite and comments on the assemblage phillipsite-clinoptilolite-mordenite: in *Natural Zeolites,* L. B. Sand and F. A. Mumpton, eds., 337–344.

Hawkins, D. B. (1981) Kinetics of glass dissolution and zeolite formation under hydrothermal conditions: *Clays & Clay Minerals* **29,** 331–340.

Hay, R. L. (1966) Zeolites and zeolite reactions in sedimentary rocks: *GSA Special Paper* **85.**

Hay, R. L. (1978) Geologic occurrence of zeolites: in *Natural Zeolites,* L. B. Sand and F. A. Mumpton, eds., Pergamon Press, New York, 135–143.

Hay, R. L. (1986) Geologic occurrence of zeolites and some associated minerals: *Pure and Applied Chemistry* **58,** 1339–1342.

Hemley, J. J. (1959) Some mineralogical equilibria in the system K_2O-Al_2O_3-SiO_2-H_2O: *Amer. J. Sci.* **257,** 241–270.

Hess, P. C. (1966) Phase equilibria of some minerals in the K_2O-Al_2O_3-SiO_2-H_2O system at 25°C and 1 atmosphere: *Amer. J. Sci.* **264,** 289–309.

Hower, J., Eslinger, E. V., Hower, M., and Perry, E. A. (1976) Mechanism of burial metamorphism of argillaceous sediments: I. Mineralogical and chemical evidence: *Geological Society of America Bulletin* **87,** 725–737.

Kodama, H. (1966) The nature of the component layers of rectorite: *Amer. Mineral.* **51,** 1035–1055.

Matsuda, T. and Henmi, K. (1983) Syntheses and properties of regularly interstratified 25 Å minerals: *Clay Science* **6,** 51–66.

Merck AG, E. (1966) *Organische reagenzien für die anorganische analyse:* Verlag Chemie GMBH, Weinheim, Germany.

Moore, D. M. and Reynolds, Jr., R. C. (1989) *X-ray Diffraction and the Identification and Analysis of Clay Minerals,* Oxford University Press, New York.

Pawloski, G. A. (1985) Quantitative determination of mineral content of geologic samples by X-ray diffraction: *Amer. Mineral.* **70,** 663–667.

Pevear, D. R., Williams, V. E., and Mustoe, G. E. (1980) Kaolinite, smectite, and K-rectorite in bentonites: Relation to coal rank at Tulameen, British Columbia: *Clays & Clay Minerals* **28,** 241–254.

Snyder, R. L. and Bish, D. L. (1989) Quantitative analysis: in *Modern Powder Diffraction, Reviews in Mineralogy* **20,** D. L. Bish and J. E. Post, eds., Mineralogical Society of America, Washington, D.C., 101–142.

Varian (1979) Analytical methods for flame spectroscopy: *Varian Techtron Pty. Ltd.,* Springvale, Australia.

Velde, B. (1985) Clay minerals, A physico-chemical explanation of their occurrence: *Developments in Sedimentology* **40,** Elsevier, New York.

Whitney, G. and Northrop, H. R. (1988) Experimental investigation of the smectite to illite reaction: Dual reaction mechanisms and oxygen-isotope systematics: *Amer. Mineral.* **73,** 77–90.

(Received 30 December 1992; accepted 30 March 1993; Ms. 2301)